© SEP 2026 | IRE Journals | Volume 10 Issue 3 | ISSN: 2456-8880
DOI: https://doi.org/10.64388/IREV10I3-1722854

Heat Transfer Analysis of Non-Newtonian Nanofluids Across a Horizontal Porous Surface Under Chemical Reaction

K.M MANJULA
Department of Mathematics, Government First Grade College, Channarayapatna, Karnataka, India.

***Abstract-** This work investigates the heat transfer behavior of ordinary Williamson and Williamson nanofluid flows over a horizontal porous surface under the influence of magnetic fields, solar radiation, binary chemical reactions, and activation energy. A mathematical model incorporating thermophoresis and Brownian motion is developed, and the governing boundary value problems are solved numerically using the shooting method. Comparative analysis of temperature profiles and heat transfer rates is presented through graphs and tables. The results demonstrate that Williamson nanofluids exhibit superior thermal performance owing to the inclusion of nanoparticles, underscoring their potential for diverse industrial applications. This study investigates the influence of cross-diffusion phenomena on the three-dimensional flow and heat transfer characteristics of a Jeffrey nanofluid confined within a Lorentz force driven stretchable channel. The rheological behavior of the non-Newtonian Jeffrey fluid model is incorporated to account for relaxation and retardation effects, while the impact of an applied magnetic field introduces magnetohydrodynamic (MHD) forces into the system. The thermal analysis considers nonlinear radiation to capture high-temperature effects, and cross-diffusion mechanisms are modeled through the Soret and Dufour effects to describe coupled heat and mass transport. The resulting boundary value problem is solved numerically to examine the effects of key physical parameters on velocity, temperature, and concentration distributions. The cross-diffusion analysis demonstrates that an increase in the Dufour number significantly augments the temperature and velocity profiles due to energy flux induced by concentration gradients, while simultaneously diminishing the concentration distribution. In contrast, elevated values of the Soret number enhance both the concentration and velocity fields by intensifying mass diffusion driven by thermal gradients within the boundary layer.*

I. INTRODUCTION

In modern research, understanding the mechanisms of non-Newtonian materials has become a focal point. The rheological characteristics of non-Newtonian materials significantly differ from those of Newtonian materials. Various substances such as shampoos, toothpaste, soaps, honey, sugar solutions, polymers, blood, ketchup, applesauce, drilling muds, and lubricants fall under the category of non-Newtonian fluids. All these liquids exhibits various rheological properties and mechanisms. In non-Newtonian fluids, pseudoplastic fluids stand out as among the most commonly encountered types. The Williamson fluid represents a pseudoplastic type of non-Newtonian fluid characterized by shear-thinning behavior. The Williamson fluid holds significant importance due to its applications in various fields including lubricants, biomedical fluids, emulsions, and nuclear fuel slurries. Williamson [1] explained the flow behavior of pseudoplastic materials and introduced a model to describe their characteristic flow. Experimental validation confirmed, the viscosity decrease with increasing rate of shear stress. Lyubimov and Perminov [2] investigated the effects of gravitational force on a thin layer of Williamson fluid. Nadeem et al. [3] formulated a model where they considered chyme as a Williamson fluid, and they conducted the flow analysis within the annular region created by two concentric tubes. Vajravelu and Dhivya [4] conducted a numerical analysis of Williamson fluid flow over a moving vertical cylinder with variable porosity using the Crank-Nicholson method. Salawu [5] numerically analyzed the stagnation-point flow with considering the influence of activation energy within a Williamson fluid comprising tiny particles over an expansive plate.

The present study investigates the MHD flow of a Williamson nanofluid across an exponential stretching surface, taking into account nonlinear thermal radiation to enhance heat transfer. While stretching scenarios have been extensively analyzed with linear thermal radiation, there has been limited attention given to flow situations involving nonlinear thermal radiation. However, the impact of thermal radiation plays a crucial role in influencing the heat transfer rate and temperature distributions within the boundary layer flow of the participating fluid. This phenomenon finds various practical applications in industries such as metallurgy, manufacturing, and energy generation. Additionally, it holds significance in electronics by impacting the performance and cooling of electronic components. Notably, one of the most notable practical uses of this concept is in utilizing solar radiation as an energy source on Earth. The study conducted by Rashidi et al. [6] examined the MHD stretched flow of a nanofluid under the influence of buoyancy and thermal radiation. A salient feature of thermal radiation in nanofluid unsteady flow over a stretching sheet was reported by Das et al. [7], the study examined the impact of thermal radiation in a time-dependent magnetohydrodynamic flow with varying viscosity. Mahanthesh et al. [8] conducted an investigation into the radiative flow of a hydromagnetic nano-fluid over the rotation of a disk. Their analysis included a nano-fluid composed of water-based nanoparticles, considering various shapes of nanoparticles such as lamina, column, sphere, tetrahedron, and hexahedron. Khan et al [9] explored a mathematical model for entropy generation incorporating variable fluid properties. They further examined the impact of mixed convection and nonlinear radiation. Reddy et al. [10] conducted a comprehensive examination of radiative heat transfer in Casson nanofluid, while also considering the viscous dissipation and particle movement. Moreover, recent research efforts have expanded beyond examining individual components to provide a complete understanding of thermal radiation's influence on various flows [11-18]. These studies provide a comprehensive understanding of the various impacts of thermal radiation in diverse fluid dynamics situations.

The motion of Williamson liquid combined with chemical reactions has found extensive applications in various fields such as drying processes, geothermal reservoirs, surface dehydration, enhanced oil recovery, geothermal pools, fibrous insulation, food processing, thermal insulation, iron rusting, fog formation, nuclear reactor cooling, synthetic materials, and numerous others. Due to extensive applications, the consequence of chemical reaction has been investigated and reported by many researchers Mukhopadhyay et al [19], Hayat et al. [20], Umavathi et al. [21], Mustafa et al. [22], Majeed et al. [23] and Nadeem et al [24].

Common liquids are often underutilized in various scientific and technical sectors due to their poor heat conductivity. However, nanoparticles are gaining significant attention in this era due to their remarkable thermal impact and unique applications across industries, biological, and engineering sectors. Such as nuclear power, paper production, insolation collectors, glass-fibre manufacture, geothermal energy pipe cooling systems, and heat transmission in aircraft apparatus. Nanoparticles, characterized by their small metallic particles ranging from 1 to 100 nm, possess enhanced thermo-physical properties. Recent studies have highlighted that nanofluids exhibit higher thermal conductivity compared to conventional fluids. Choi [25] provided experimental validation of nanofluids, establishing the existence of this concept. Throughout the last two decades, researchers around the world have been fascinated by the exceptional properties of nanofluid, remarkable studies being recorded in the field [26-34].

The flow and heat transfer characteristics of non-Newtonian fluids, such as Williamson fluids, are of significant interest due to their complex rheological behavior. When these fluids are enhanced with nanoparticles, forming nanofluids, their thermal properties are further improved. This study focuses on the comparative analysis of Williamson and Williamson nanofluid flows across a horizontal porous surface in the presence of magnetic fields, solar radiation, binary chemical reactions and activation energy. The presenting governing equations are highly nonlinear mathematical expressions that are numerically treated to examine

© SEP 2026 | IRE Journals | Volume 10 Issue 3 | ISSN: 2456-8880
DOI: https://doi.org/10.64388/IREV10I3-1722854

the outcomes. Graphical representations are employed and discussed to express the mechanisms underlying various physical constraints on dimensionless quantities. The numerical computations cover two distinct scenarios: Williamson nanofluid and ordinary Williamson fluid. The results reveal a notably higher heat transfer rate for the Williamson nanofluid in comparison to the ordinary Williamson fluid.

Mathematical Formulation

We consider a steady two-dimensional flow of Williamson fluid containing nanoparticles over an exponentially stretching surface. The flow configuration with the adopted coordinate system is shown in Figure 1, where the x-axis is taken along the stretching surface in the direction of motion and the y-axis is normal to it. The surface is exponentially stretched in the x-direction with a velocity $U_w(x) = U_0 e^{x/L}$. A magnetic field strength B_0 is applied along the y-direction. At the surface, the temperature and nanoparticle volume fraction of the nanofluid are denoted as T_w and C_w , respectively.

With all above assumptions the governing boundary layer equations are:

$$\frac{\partial u}{\partial x} + \frac{\partial v}{\partial y} = 0, \tag{1}$$

$$u\frac{\partial u}{\partial x} + v\frac{\partial u}{\partial y} = \nu\frac{\partial^2 u}{\partial y^2} + \sqrt{2}\nu\Gamma\frac{\partial u}{\partial y}\frac{\partial^2 u}{\partial y^2} - \frac{\sigma B_0^2}{\rho}u - \frac{\nu}{k'}u$$
$$+g(\beta_0(T - T_\infty) + \beta_1(T - T_\infty)^2 + \beta_2(C - C_\infty)) \tag{2}$$

$$u\frac{\partial T}{\partial x} + v\frac{\partial T}{\partial y} = \alpha_m\frac{\partial^2 T}{\partial y^2} + \tau\left[D_m\frac{\partial C}{\partial y}\frac{\partial T}{\partial y} + \frac{D_T}{T_\infty}\left(\frac{\partial T}{\partial y}\right)^2\right] + \frac{Q_0}{\rho c_p}(T - T_\infty) - \frac{1}{\rho c_p}\frac{\partial q_r}{\partial y} \tag{3}$$

$$u\frac{\partial C}{\partial x} + v\frac{\partial C}{\partial y} = D_m\frac{\partial^2 C}{\partial y^2} + \frac{D_T}{T_\infty}\frac{\partial^2 T}{\partial y^2} - k_r^2(C - C_\infty)\left(\frac{T}{T_\infty}\right)^m \exp\left(-\frac{E_a}{\kappa T}\right), \tag{4}$$

The radiative heat flux expression in equation (3) is given by the Rosseland approximation as;

$$q_r = -\frac{4\sigma^*}{3k^*}\frac{\partial T^4}{\partial y} = -\frac{16\sigma^*}{3k^*}T^3\frac{\partial T}{\partial y} \tag{5}$$

Where σ^* and k^* are the Stefan-Boltzman constant and the mean absorption coefficient correspondingly, and in view to equation (5) in equation (3) reduces to

$$u\frac{\partial T}{\partial x} + v\frac{\partial T}{\partial y} = \alpha_m\frac{\partial^2 T}{\partial y^2} + \tau\left[D_m\left(\frac{\partial C}{\partial y}\frac{\partial T}{\partial y}\right) + \frac{D_T}{T_\infty}\left(\frac{\partial T}{\partial y}\right)^2\right] + \frac{Q_0}{\rho c_p}(T - T_\infty)$$
$$+\frac{16\sigma^*}{3\rho c_p k^*}\left[T^3\frac{\partial^2 T}{\partial y^2} + 3T^2\left(\frac{\partial T}{\partial y}\right)^2\right] \tag{6}$$

The boundary conditions considered for the present flow analysis are;

$$u = U_w(x) = U_0 e^{x/L}, \quad v = 0, \quad T = T_w, \quad C = C_w \quad \text{at} \quad y = 0,$$
$$u = 0, \quad T \to T_\infty, \quad C \to C_\infty \quad as \quad y \to \infty. \tag{7}$$

The term $k_r^2 (C - C_\infty) \left(\frac{T}{T_\infty}\right)^m \exp\left(-\frac{E_a}{\kappa T}\right)$ in equation (4) represents the modified Arrhenius equation in which k_r^2 is the reaction rate, E_a the activation energy, $\kappa = 8.61 \times 10^{-5} eV/K$ the Boltzmann constant and m the fitted rate constant which generally lies in the range $-1 < m < 1$. where u and v are velocity components along x and y directions respectively, T and C are temperature and volume fraction of nanoparticles correspondingly, ν -kinematic viscosity, ρ -is density of the fluid, Q_0 -dimensional heat source coefficient, B_0-magnetic field, k' -permeability of the porous medium, $\alpha_m = k/\rho c_p$ -thermal diffusivity of the fluid, k -thermal conductivity of the fluid, D_T -thermophoretic diffusion coefficient, D_m -Brownian diffusion coefficient, $\tau = (\rho c)_p/(\rho c)_f$ -ratio of the effective heat capacity of the nanoparticle to that of an ordinary fluid, $(\rho c)_f$ and $(\rho c)_p$ are heat capacities of the ordinary fluid and nanoparticles respectively, T_∞ and C_∞ are ambient temperature and volume fraction of nanoparticles respectively and q_r radiative heat flux.

Now, introduce the following similarity transformations

$$u = U_0 e^{\frac{x}{L}} f'(\eta), \; v = -\sqrt{\frac{U_0 \nu}{2L}} e^{\frac{x}{2L}} \left(f(\eta) + \eta f'(\eta)\right), \; \eta = \sqrt{\frac{U_0}{2\nu L}} e^{x/2L} y$$

$$T = \theta(\eta)(T_w - T_\infty) + T_\infty, \; C = \phi(\eta)(C_w - C_\infty) + C_\infty \tag{8}$$

With the help of above transformations, equation Eq. (1) is identically satisfied and Equation's. (2), (4) and (6) along with boundary conditions (7) take the following equations;

$$f''' + ff'' - 2(f')^2 + \omega f'' f''' - (M + kp)f' + \gamma(1 + \gamma_1)(\theta + \alpha\theta^2 + N\phi) = 0, \tag{9}$$

$$\theta'' + R\left[\left(1 + (\theta_w - 1)\theta(\eta)\right)^3 \theta''(\eta) + 3(\theta_w - 1)\theta'^2(\eta)\left(1 + (\theta_w - 1)\theta(\eta)\right)^2\right]$$
$$\Pr\{f\theta' + Nb\phi'\theta' + Nt(\theta')^2 + Q\theta\} = 0 \tag{10}$$

$$\phi'' + Lef\phi' + \frac{Nt}{Nb}\theta'' - Le\sigma(1 + \delta\theta)^m \phi \exp\left(-\frac{E}{1 + \delta\theta}\right) = 0, \tag{11}$$

and the corresponding boundary conditions become;

$$f(0) = 0, \quad f'(0) = 1, \quad \theta(0) = 1, \quad \phi(0) = 1,$$
$$f'(\infty) = 0, \qquad \theta(\infty) = 0, \quad \phi(\infty) = 0. \tag{12}$$

where $\omega = \Gamma\sqrt{\frac{U_0^3 e^{3x/L}}{\nu L}}$ -Williamson fluid Parameter, $M = \frac{2L\sigma B_0^2}{\rho U_w}$ -magnetic field parameter, $kp = \frac{2L\nu}{k' U_w}$ -porous parameter $Pr = \frac{\nu}{\alpha_m}$ -Prandtl number, $R = \frac{16\sigma^* T_\infty^3}{3k k^*}$ -radiation parameter, $\theta_w = \frac{T_w}{T_\infty}$ -temperature parameter, $Nb = \frac{D_m(C_w - C_\infty)}{\nu}$ -Brownian motion parameter, $Nt = \frac{\tau D_T(T_w - T_\infty)}{T_\infty \nu}$ -thermophoresis parameter, $Le = \frac{\nu}{D_m}$ -Lewis number and $Q = \frac{Q_0 2L}{\rho c_p U_w}$ –heat generation parameter, $\sigma = -\frac{k_r^2 2L}{U_w}$ -dimensionless reaction rate, $\delta = \frac{T_w - T_\infty}{T_\infty}$ - the temperature difference parameter, $E = \frac{E_a}{\kappa T_\infty}$- non-dimensional activation energy.

The Skin friction coefficient, Nusselt number and Sherwood numbers are;

$$C_f = \frac{\tau_w}{\rho U_w^2}, \quad Nu_x = \frac{x q_w}{k(T_w - T_\infty)}, \quad Sh_x = \frac{x q_m}{D_B(C_w - C_\infty)} \tag{13}$$

Where τ_w -surface shear stress, q_w -surface heat flux and q_m -surface mass flux are given by;

$$\tau_w = \mu\left(\frac{\partial u}{\partial y} + \frac{\Gamma}{2}\left(\frac{\partial u}{\partial y}\right)^2\right)_{y=0}$$
$$q_w = -k\left(\frac{\partial T}{\partial y} + q_r\right)_{y=0},$$
$$q_m = -D_m\left(\frac{\partial c}{\partial y}\right)_{y=0} \tag{14}$$

Now through merging equation (8) and (14) in interpretation of equation (13), we have obtained;

$$\sqrt{Re_x} C_f = \left(f''(0) + \frac{\lambda}{2} f''(0)^2\right),$$
$$\frac{Nu_x}{\sqrt{2Re}} = -\frac{x}{2L}(1 + R\theta_w^3)\theta'(0),$$
$$\frac{Sh_x}{\sqrt{2Re}} = -\frac{x}{2L}\phi'(0). \tag{15}$$

Where $Re_x = \frac{U_0 L}{\nu}$ is the local Reynolds number.

II. PHYSICAL INTERPRETATION

In this section, a comprehensive numerical investigation is carried out to examine the influence of the governing physical parameters on the flow, thermal, and nanoparticle transport characteristics. Particular attention is given to the velocity f'(η), temperature θ(η), and nanoparticle volume fraction ϕ(η) profiles. The numerical results are presented through graphical illustrations and tables, and the corresponding physical mechanisms are discussed in detail. Unless otherwise stated, the remaining governing parameters are maintained at their prescribed default values, which are specified in the respective figures. Figures 2 and 3 illustrate the influence of the magnetic parameter M on the velocity and temperature distributions, respectively. As M increases from 0.5 to 2, a clear reduction in the velocity profile is observed, accompanied by an increase in the temperature profile. The decrease in velocity is attributed to the enhanced Lorentz force generated by the interaction between the applied magnetic field and the electrically conducting fluid. This resistive electromagnetic force acts against the fluid motion and consequently suppresses the momentum transport, resulting in a thinner momentum boundary layer. On the other hand, the reduction in fluid motion weakens the convective transport of thermal energy away from the surface. Consequently, heat accumulates within the boundary layer, leading to an increase in the temperature and a corresponding thickening of the thermal boundary layer. Figure 4 presents the effect of the permeability parameter on the velocity distribution $f'(\eta)$. It is evident that increasing the permeability parameter causes a reduction in the fluid velocity. The porous medium offers additional resistance to the fluid motion, thereby restricting the movement of the fluid through the porous structure. As the resistance offered by the porous matrix becomes stronger, the fluid motion is increasingly suppressed, resulting in a reduction in the velocity profile and momentum transport within the boundary layer. The corresponding influence of the permeability parameter on the temperature profile $\theta(\eta)$ is displayed in Figure 5. An enhancement in both the temperature profile and thermal boundary-layer thickness is observed with increasing permeability parameter. The increased resistance to fluid motion reduces the convective transport of heat from the surface into the surrounding fluid. As a result, the removal of thermal energy becomes less effective, causing heat to be retained near the surface and consequently increasing the temperature distribution. Figures 6 and 7 depict the effects of the Brownian motion parameter Nb on the temperature and nanoparticle volume-fraction profiles, respectively. An increase in Nb produces a noticeable enhancement in the temperature profile and thermal boundary-layer thickness. This behavior can be attributed to the intensified random motion of nanoparticles, which increases microscopic interactions between the nanoparticles and the base fluid and thereby modifies the thermal transport mechanism. In contrast, the nanoparticle volume-fraction profile decreases as Nb increases, as observed in Figure 7. The stronger Brownian diffusion promotes the redistribution of nanoparticles away from the surface region, resulting in a reduction in the local nanoparticle concentration within the boundary layer. Thus, Brownian motion plays an important role in coupling nanoparticle diffusion with heat transport.

Figures 8 and 9 demonstrate the effects of the thermophoresis parameter Nt on the temperature and nanoparticle volume-fraction distributions, respectively. Increasing Nt leads to an enhancement in both temperature and nanoparticle volume-fraction profiles. The thermophoretic effect induces nanoparticle migration in response to the temperature gradient, generally driving particles from regions of higher temperature toward regions of lower temperature. This migration modifies the nanoparticle distribution and enhances the interaction between nanoparticle transport and thermal energy transfer. Consequently, the thermal and nanoparticle boundary layers become more pronounced as the thermophoresis parameter increases. Figure 10 illustrates the effect of the thermal radiation parameter R on the temperature distribution. It is observed that increasing R results in higher temperature values and a thicker thermal boundary layer. The presence of thermal radiation provides an additional mode of energy transport within the fluid, thereby increasing the overall thermal energy available in the boundary layer. Consequently, the temperature of the fluid increases and the thermal boundary layer becomes thicker. This result highlights the significance of radiative heat transfer in high-temperature thermal transport applications. Finally, Figure 11 presents the influence of the Lewis number Le on the nanoparticle volume-fraction profile. The nanoparticle concentration decreases progressively with increasing Le. Since the Lewis number represents the relative importance of thermal diffusivity to mass or nanoparticle diffusivity, a larger Le corresponds to weaker nanoparticle mass diffusion relative to thermal diffusion. Consequently, nanoparticle transport becomes less effective, leading to a reduction in the nanoparticle volume-fraction distribution and a thinner concentration boundary layer. This behavior confirms the important role of the Lewis number in controlling nanoparticle diffusion and concentration transport within the boundary layer.

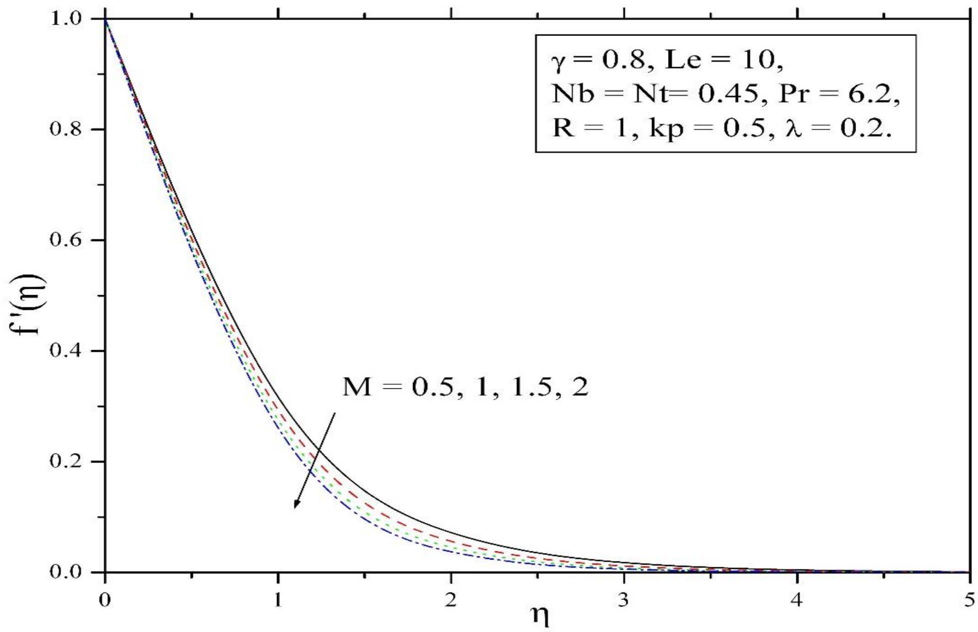

Figure 1: Effect of M on $f'(\eta)$

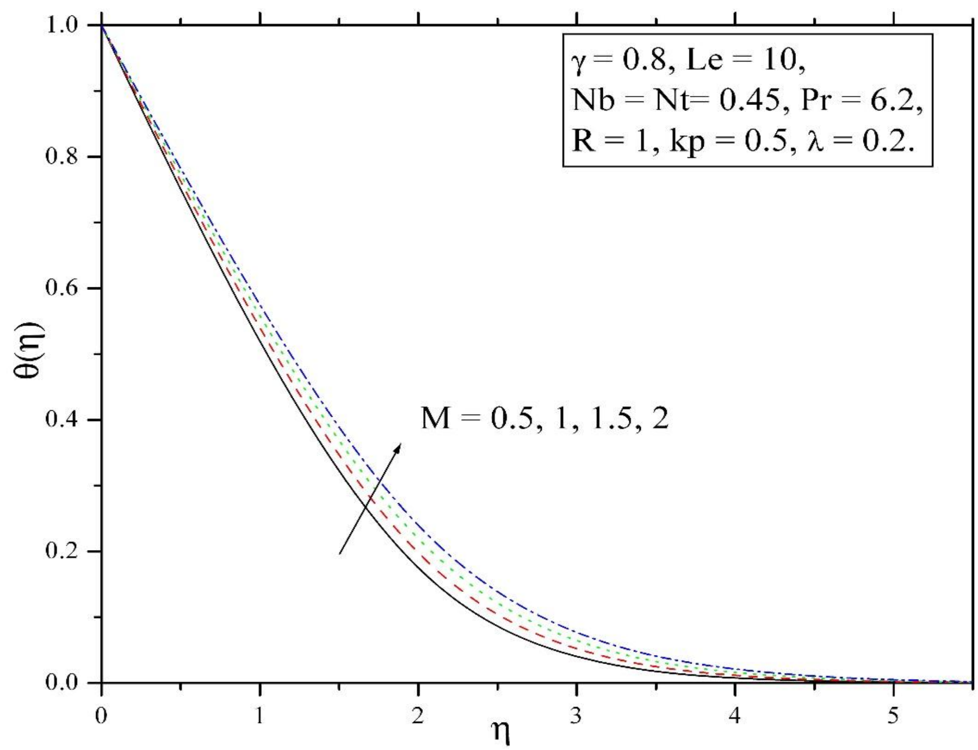

Figure 2: Effect of M on $\theta(\eta)$

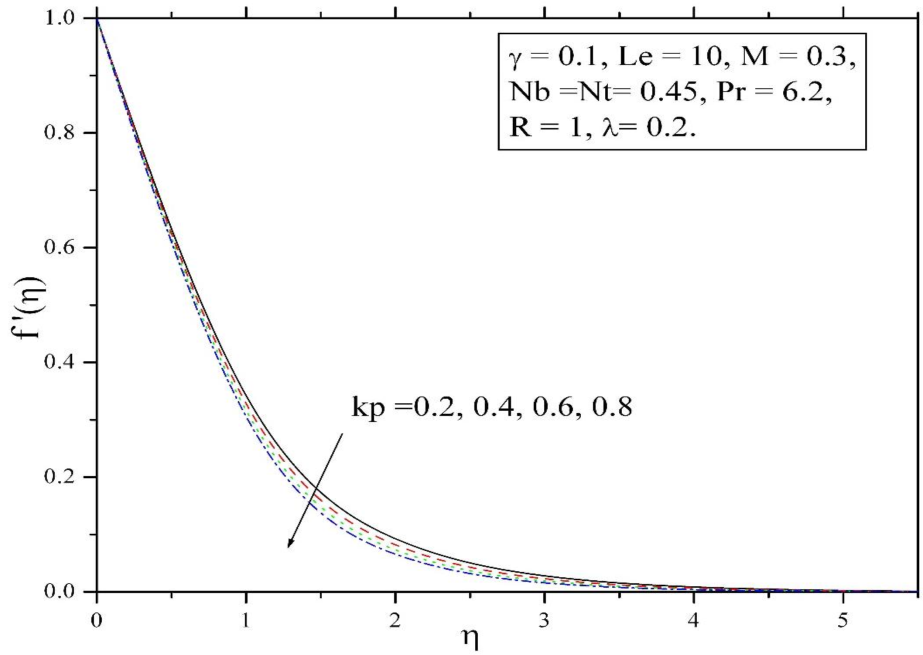

Figure 3: Effect of Kp on $f'(\eta)$.

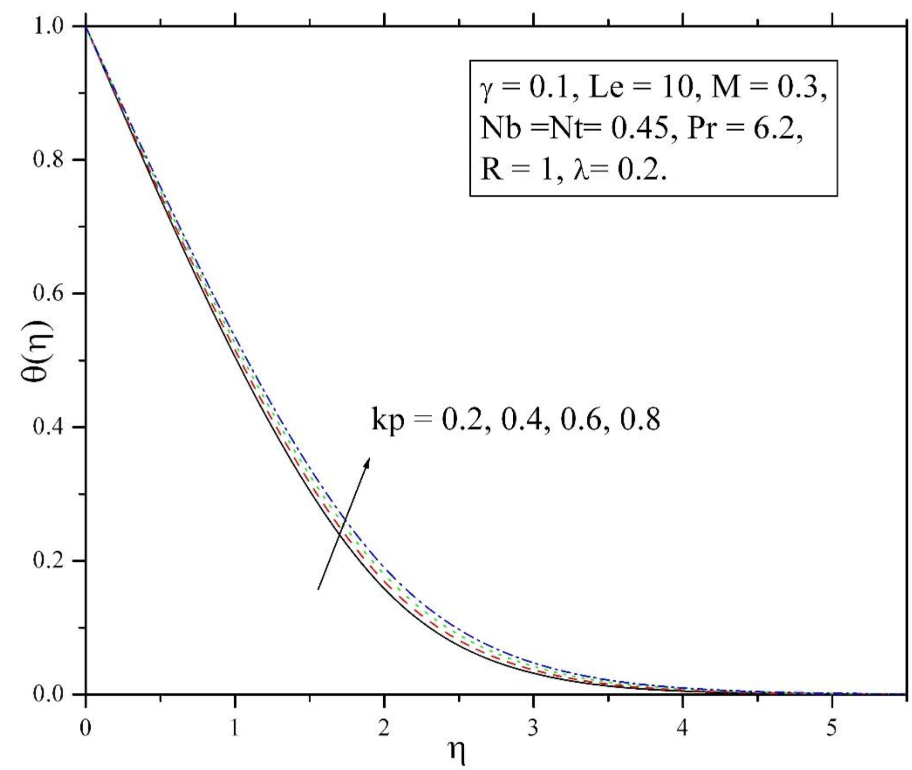

Figure 4: Effect of kp on $\theta(\eta)$.

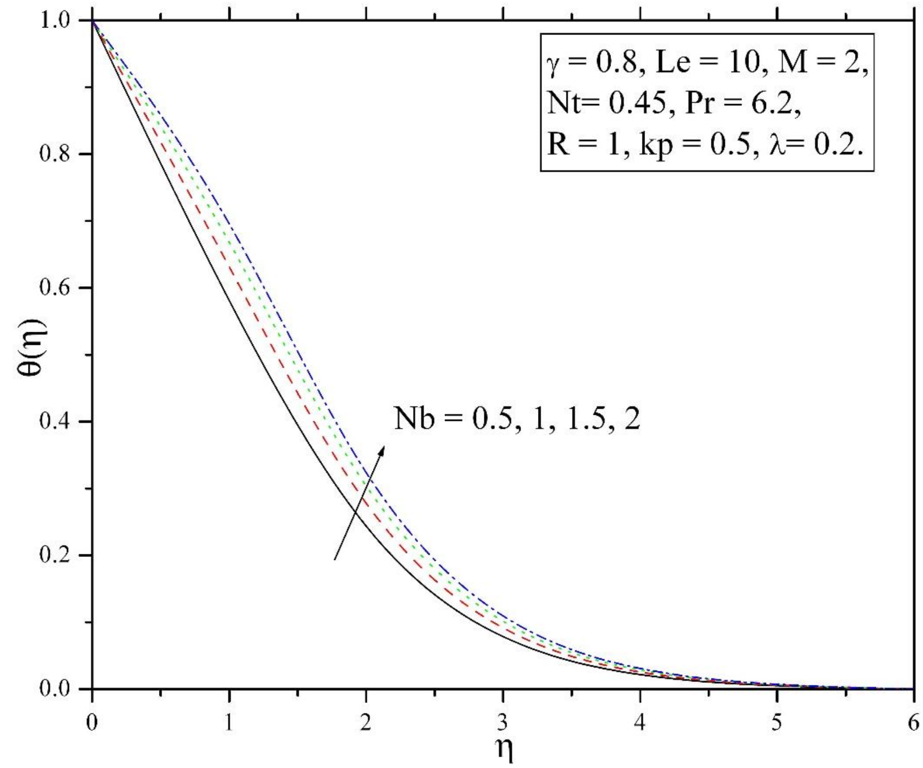

Figure 5: Effect of Nb on $\theta(\eta)$.

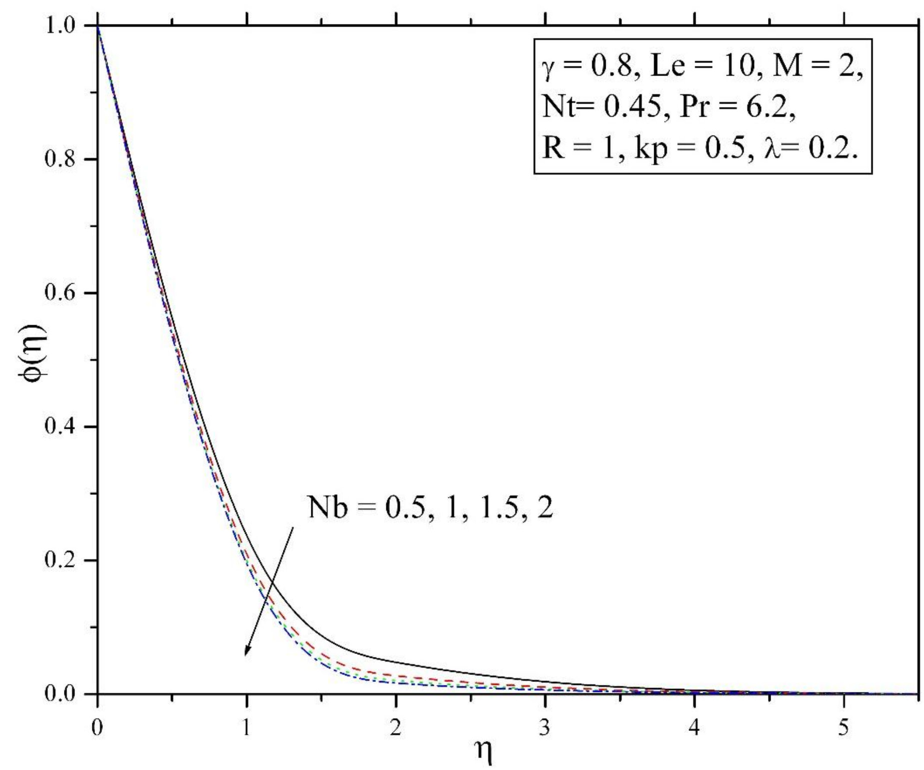

Figure 6: Effect of Nb on $\phi(\eta)$.

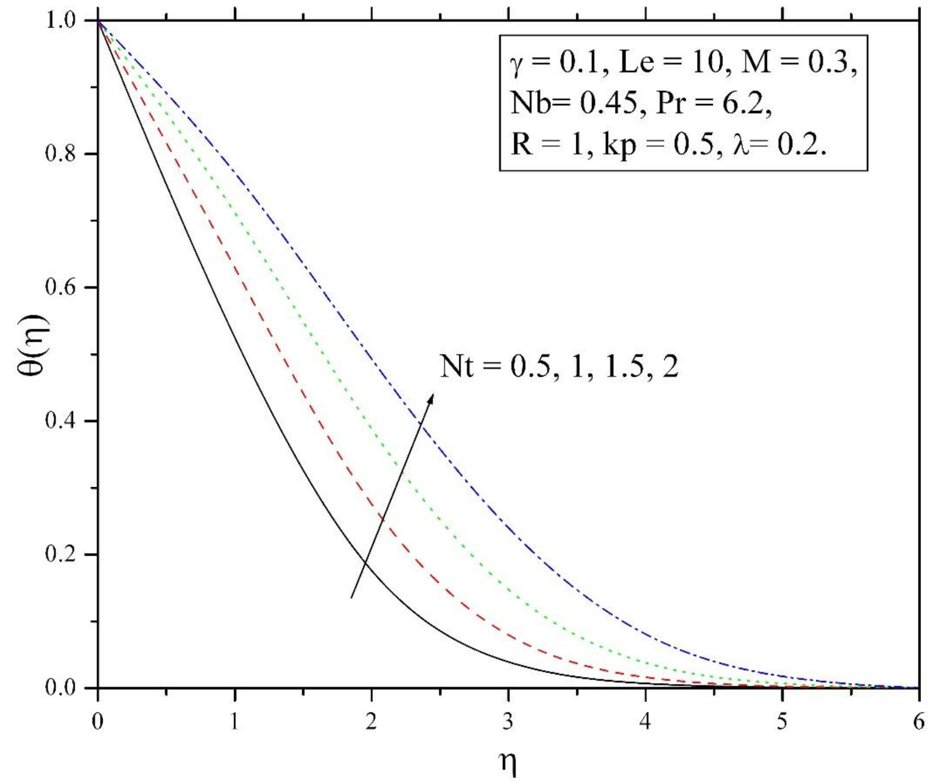

Figure 7: Effect of Nt on $\theta(\eta)$.

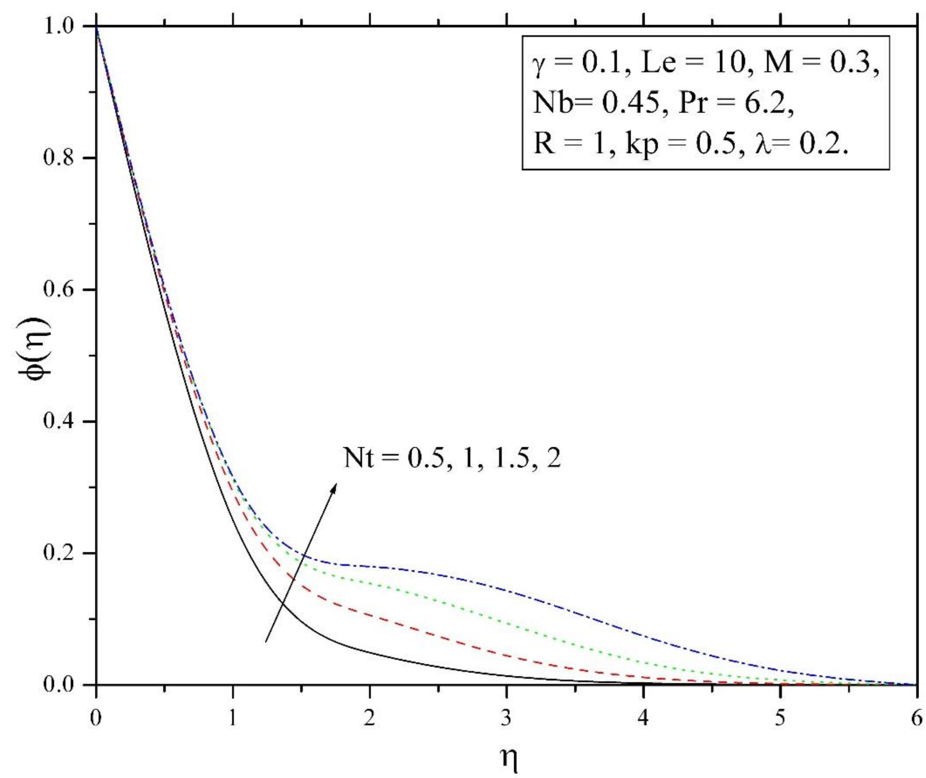

Figure 8: Effect of Nt on $\phi(\eta)$.

© SEP 2026 | IRE Journals | Volume 10 Issue 3 | ISSN: 2456-8880
DOI: https://doi.org/10.64388/IREV10I3-1722854

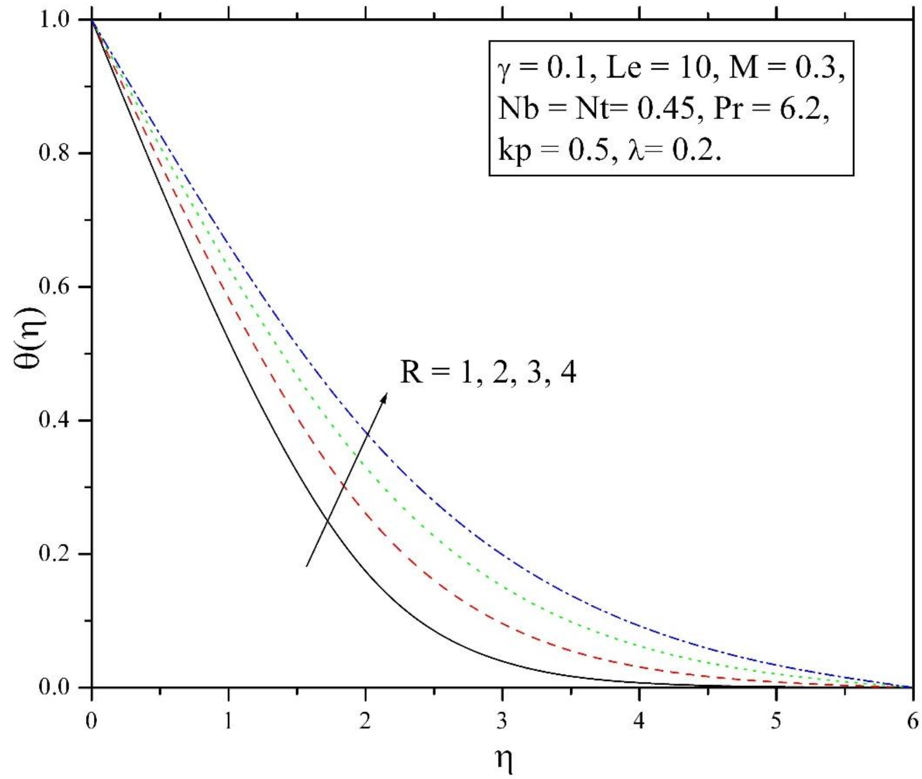

Figure 9: Effect of R on $\theta(\eta)$.

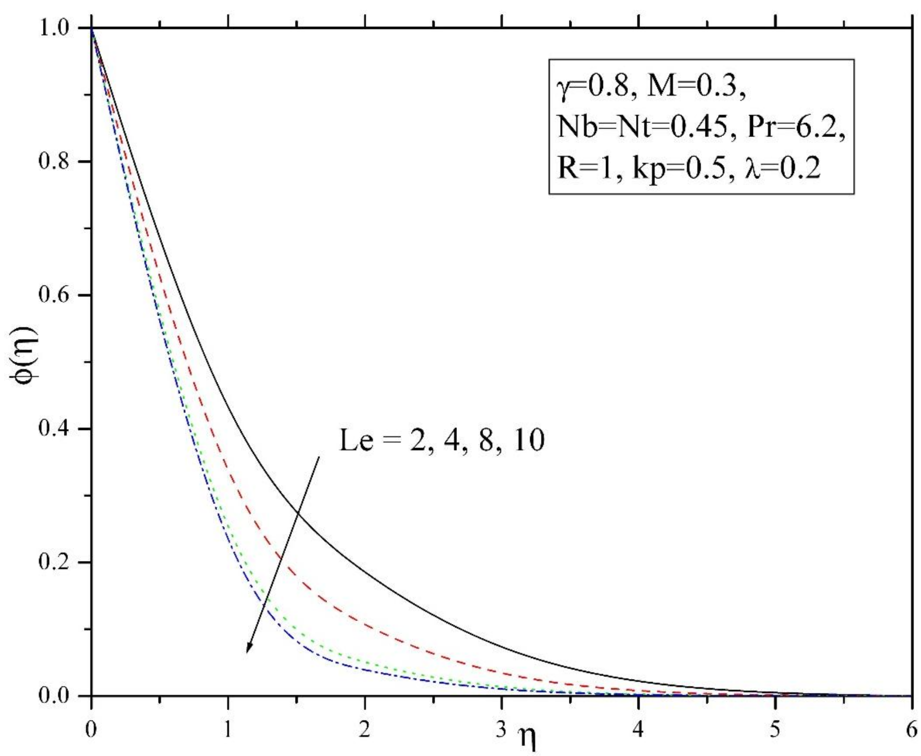

Figure 10: Effect of Nb on $\phi(\eta)$.

III. CONCLUDING REMARKS

The present study numerically investigates the MHD flow, heat transfer, and nanoparticle transport characteristics in a porous medium under the influence of magnetic field, permeability, Brownian motion, thermophoresis, thermal radiation, and Lewis number. The results reveal that increasing the magnetic parameter M significantly suppresses the velocity due to the enhanced Lorentz force, while the temperature increases because of the reduced convective heat transport. Similarly, increasing the permeability parameter increases the resistance offered by the porous medium, leading to a reduction in velocity and an enhancement in temperature. The Brownian motion parameter Nb enhances the temperature distribution and thermal boundary-layer thickness, whereas it reduces the nanoparticle volume-fraction profile due to intensified nanoparticle diffusion. An increase in the thermophoresis parameter Nt enhances both temperature and nanoparticle volume-fraction distributions by promoting nanoparticle migration along the temperature gradient. Furthermore, increasing the thermal radiation parameter R increases the temperature and thermal boundary-layer thickness owing to the additional radiative heat transfer. In contrast, increasing the Lewis number Le decreases the nanoparticle volume-fraction profile because of the reduced nanoparticle mass diffusivity relative to thermal diffusivity. Overall, the results demonstrate that magnetic and porous-medium effects predominantly control momentum transport, while Brownian motion, thermophoresis, thermal radiation, and Lewis number play significant roles in regulating heat and nanoparticle transport. These findings may be useful in the design and optimization of thermal management systems and porous-media applications involving nanofluids.

REFERENCES

[1] Williamson, R. Vo. "The flow of pseudoplastic materials." *Industrial & Engineering Chemistry* 21, no. 11 (1929): 1108-1111. Crossref

[2] Lyubimov, D. V., and A. V. Perminov. "Motion of a thin oblique layer of a pseudoplastic fluid." *Journal of Engineering Physics and Thermophysics* 75, no. 4 (2002): 920-924.

[3] Nadeem, S., Ashiq, S., and Ali, M. "Williamson fluid model for the peristaltic flow of chyme in small intestine." *Mathematical Problems in Engineering*, (2012). Crossref

[4] Dhivya M and Vajravelu K. "Heat transfer characteristics of a Williamson fluid flow through a variable porosity regime." *International Journal of Ambient Energy*, 44, no. 1 (2023).

[5] Salawu, S. O. "Stagnation-point flow of Williamson fluid along a stretched plate with convective thermal condition and activation energy." *International Journal of Applied Mechanics and Engineering* 28, no. 3 (2023).

[6] Rashidi, M. M., N. Vishnu Ganesh, AK Abdul Hakeem, and B. Ganga. "Buoyancy effect on MHD flow of nanofluid over a stretching sheet in the presence of thermal radiation." *Journal of Molecular liquids* 198 (2014): 234-238. Crossref

[7] Das, Kalidas, Pinaki Ranjan Duari, and Prabir Kumar Kundu. "Nanofluid flow over an unsteady stretching surface in presence of thermal radiation." *Alexandria engineering journal* 53, no. 3 (2014): 737-745. Crossref

[8] Mahanthesh, B., B. J. Gireesha, S. A. Shehzad, A. Rauf, and PB Sampath Kumar. "Nonlinear radiated MHD flow of nanoliquids due to a rotating disk with irregular heat source and heat flux condition." *Physica B: Condensed Matter* 537 (2018): 98-104. Crossref

[9] Khan, M. Ijaz, T. Hayat, M. Imran Khan, M. Waqas, and A. Alsaedi. "Numerical simulation of hydromagnetic mixed convective radiative slip flow with variable fluid properties: a mathematical model for entropy generation." *Journal of Physics and Chemistry of Solids* 125 (2019): 153-164. Crossref

[10] Reddy, Y. Dharmendar, B. Shankar Goud, Ali J. Chamkha, and M. Anil Kumar. "Influence of radiation and viscous dissipation on MHD heat transfer Casson nanofluid flow along a nonlinear stretching surface with chemical reaction." *Heat Transfer* 51, no. 4 (2022): 3495-3511. Crossref

[11] Pal, Dulal, and Hiranmoy Mondal. "Influence of temperature-dependent viscosity and thermal radiation on MHD forced convection over a non-isothermal wedge." *Applied Mathematics and Computation* 212, no. 1 (2009): 194-208. Crossref

[12] Makinde, Oluwole Daniel. "Chemically reacting hydromagnetic unsteady flow of a radiating fluid past a vertical plate with constant heat flux." *Zeitschrift für Naturforschung A* 67, no. 5 (2012): 239-247. Crossref

[13] Shehzad, Sabir Ali, Tasawar Hayat, Ahmed Alsaedi, and Mustafa Ali Obid. "Nonlinear thermal radiation in three-dimensional flow of Jeffrey nanofluid: a model for solar energy." *Applied Mathematics and Computation* 248 (2014): 273-286.

[14] Raju, C. S. K., S. M. Ibrahim, S. Anuradha, and P. Priyadharshini. "Bio-convection on the nonlinear radiative flow of a Carreau fluid over a moving wedge with suction or injection." *The European Physical Journal Plus* 131 (2016): 1-16. Crossref

[15] Sajjan, Kiran, Nehad Ali Shah, N. Ameer Ahammad, C. S. K. Raju, M. Dinesh Kumar, and Wajaree Weera. "Nonlinear Boussinesq and Rosseland approximations on 3D flow in an interruption of Ternary nanoparticles with various shapes of densities and conductivity properties." *AIMS Math* 7, no. 10 (2022): 18416-18449.

[16] Gireesha, B. J., S. Manthesha, F. Almeida, and P. Mallikarjun. "Flow of magnetized Powell-Eyring fluid in microchannel exposed to non-linear radiation and constricted to slip regime by varying viscosity." *International Journal of Modelling and Simulation* (2023): 1-14.

[17] Anantha Kumar, K., A. C. Venkata Ramudu, V. Sugunamma, and N. Sandeep. "Effect of non-linear thermal radiation on MHD Casson fluid flow past a stretching surface with chemical reaction." *International Journal of Ambient Energy* 43, no. 1 (2022): 8400-8407. Crossref

[18] Ismail, Mohammed, and David Maxim Gururaj. "Numerical Investigation on Nonlinear Radiative Magneto Hydrodynamics Hybrid Nanofluid Flow Past a Stretching Cylinder Embedded in Porous Medium." *Journal of Nanofluids* 12, no. 3 (2023): 809-818.

[19] Mukhopadhyay, Swati, and Krishnendu Bhattacharyya. "Unsteady flow of a Maxwell fluid over a stretching surface in presence of chemical reaction." *Journal of the Egyptian Mathematical Society* 20, no. 3 (2012): 229-234. Crossref

[20] Hayat, Tasawar, Madiha Rashid, Maria Imtiaz, and Ahmed Alsaedi. "MHD convective flow due to a curved surface with thermal radiation and chemical reaction." *Journal of Molecular Liquids* 225 (2017): 482-489. Crossref

[21] Umavathi, J. C., Mikhail A. Sheremet, and Syed Mohiuddin. "Combined effect of variable viscosity and thermal conductivity on mixed convection flow of a viscous fluid in a vertical channel in the presence of first order chemical reaction." *European Journal of Mechanics-B/Fluids* 58 (2016): 98-108. Crossref

[22] Mustafa, M., Junaid Ahmad Khan, T. Hayat, and A. Alsaedi. "Buoyancy effects on the MHD nanofluid flow past a vertical surface with chemical reaction and activation energy." *International Journal of Heat and Mass Transfer* 108 (2017): 1340-1346. Crossref

[23] Majeed, A., A. Zeeshan, and R. Ellahi. "Chemical reaction and heat transfer on boundary layer Maxwell Ferro-fluid flow under magnetic dipole with Soret and suction effects." *Engineering science and technology, an international journal* 20, no. 3 (2017): 1122-1128. Crossref

[24] Nadeem, Muhammad, Imran Siddique, Irfan Saif Ud Din, Fuad A. Awwad, Emad AA Ismail, and Hijaz Ahmad. "Impact of chemical reaction on Eyring–Powell fluid flow over a thin needle with nonlinear thermal radiation." *Scientific Reports* 13, no. 1 (2023): 21401. Crossref

[25] Sus, Choi. "Enhancing thermal conductivity of fluids with nanoparticles, developments and applications of non-Newtonian flows." *ASME, FED, MD*, 1995 231 (1995): 99-I05.

[26] Muhammad, K., T. Hayat, and A. Alsaedi. "Numerical study of Newtonian heating in flow of hybrid nanofluid (SWCNTs+ CuO+ Ethylene glycol) past a curved surface with viscous

dissipation." *Journal of Thermal Analysis and Calorimetry* 143 (2021): 1291-1302.

[27] Khan, Muhammad Ijaz, Khursheed Muhammad, Tasawar Hayat, Shahid Farooq, and Ahmed Alsaedi. "Numerical simulation for Darcy-Forchheimer flow of carbon nanotubes due to convectively heated nonlinear curved stretching surface." *International Journal of Numerical Methods for Heat & Fluid Flow* 29, no. 9 (2019): 3290-3304.

[28] Ali, Asgar, R. N. Jana, and Sanatan Das. "Radiative CNT-based hybrid magneto-nanoliquid flow over an extending curved surface with slippage and convective heating." *Heat Transfer* 50, no. 3 (2021): 2997-3020.

[29] Kumbhakar, Bidyasagar, Susmay Nandi, and Ali J. Chamkha. "Unsteady hybrid nanofluid flow over a convectively heated cylinder with inclined magnetic field and viscous dissipation: A multiple regression analysis." *Chinese Journal of Physics* 79 (2022): 38-56.

[30] Ali, Aamir, Sunila Malik, M. Awais, A. S. Alqahtani, and M. Y. Malik. "MHD peristaltic flow of hybrid nanomaterial between compliant walls with slippage and radiation." *Journal of Molecular Liquids* 393 (2024): 123619.

[31] Pavan Kumar, P. L., B. J. Gireesha, and P. Venkatesh. "Impact of trihybrid nanofluid on the transient thermal performance of inclined dovetail fin with emphasis on internal heat generation." *The European Physical Journal Plus* 139, no. 1 (2024): 1-18.

[32] Manjunatha, S., V. Puneeth, B. J. Gireesha, and Ali Chamkha. "Theoretical study of convective heat transfer in ternary nanofluid flowing past a stretching sheet." *Journal of Applied and Computational Mechanics* 8, no. 4 (2022): 1279-1286.

[33] Godasiaei, Seyed Hamed, and Ali J. Chamkha. "Advancing heat transfer modeling through machine learning: A focus on forced convection with nanoparticles." *Numerical Heat Transfer, Part A: Applications* (2023): 1-23.

[34] Shao, Wenkai, M. K. Nayak, Rifaqat Ali, S. Nazari, and Ali J. Chamkha. "Simultaneous numerical examination of thermal and entropy characteristics of Al_2O_3–H_2O nanofluid within a porous diamond-shaped container with a⊥-shaped obstacle." *Case Studies in Thermal Engineering* 54 (2024): 104059.